Journal of Electronic Research and Application, 2024, Volume 8, Issue 3
http://ojs.bbwpublisher.com/index.php/JERA
ISSN Online: 2208-3510
ISSN Print: 2208-3502

Study on the Preparation, the Magnetic Performance, and the Oxygen Evolution Reaction of $LaMnO_{3+\delta}$

Peng Fan[1], Qirui Wu[1], Geming Wang[2], Rahman Sheikh Tamjidur[2], Chendong Shao[2]*

[1]Wuhan NARI Limited Liability Company, State Grid Electric Power Research Institute, NARI Group (State Grid Electric Power Research Institute) Co., Ltd., Wuhan 430074, Hubei Province, China
[2]Provincial Key Laboratory of Plasma Chemistry and Advanced Materials, Wuhan Institute of Technology, Wuhan 430073, Hubei Province, China

***Corresponding author:** Chendong Shao, 1013175079@qq.com

Abstract: In this paper, a series of $LaMnO_{3+\delta}$ (LMOs) were successfully prepared by adjusting the sintering temperature using the sol-gel method with ABO_3-type LMO oxides as the object of study. The results showed that with the increase of sintering temperature, the O_{ads}, oxygen vacancies, and Mn^{4+} content in the system gradually decreased, and the oxygen evolution reaction (OER) was subsequently weakened. Although the suitable Mn^{3+}/Mn^{4+} valence ratio (2.15:1) of the LMO700 sample created a strong ferromagnetic double-exchange effect, the high concentration of oxygen vacancies in LMO700 disturbed this effect and weakened its macro magnetism. This paper serves to contribute to the design and development of new magnetic perovskite electrocatalysts.

Keywords: Manganese oxides; Microstructure; Magnetic properties; Oxygen evolution reaction

Online publication: June 14, 2024

1. Introduction

The structural tunability of ABO_3-type manganese oxide LMOs makes these materials particularly susceptible to optimization and modification of magnetic and electrochemical properties through microstructural and electronic structure modulation [1, 2]. As far as magnetism is concerned, LMOs possess multiple couplings and competing and easily regulated magnetic orders due to the strong interactions between their spins, charges, orbitals, and lattices [3]. The optimization of transition metal oxides' microstructure through adjustments in their preparation process has garnered significant interest within the academic community. These modifications influence magnetically ordered interactions, thereby facilitating effective regulation of electron transfer and conversion during the Oxygen Evolution Reaction (OER) catalytic process.

In this paper, the effect of sintering temperature on the microstructure, magnetic, and OER properties of LMO was studied, and we successfully prepared a series of LMOs with different sintering temperatures.

2. Experiment

Firstly, the precursor was placed in a chamber furnace and heated up to 220 ℃ at a rate of 10 ℃ min^{-1} and held in an air atmosphere for 1 h. Then, the precursor was heated up to 700, 800, 900, and 1000 ℃ at a rate of 10 ℃ min^{-1} and held in an air atmosphere for 4 h and cooled down with the furnace, respectively; Finally, the $LaMnO_{3+\delta}$ powder samples were prepared at different sintering temperatures and could be obtained by grinding. We labeled them as LMO700, LMO800, LMO900 and LMO1000, respectively.

3. Experimental results and analysis

3.1. Crystal structure and surface morphology analysis

Figure 1 shows the XRD patterns of $LaMnO_{3+\delta}$ samples (LMO700, LMO800, LMO900, and LMO1000) prepared at different sintering temperatures. All samples had sharp diffraction peaks, indicating high crystallinity. There were no impurity phases, proving that single-phase LMO structures could be formed at sintering temperatures of 700, 800, 900, and 1000 °C. The sintering temperatures of 700, 800, 900, and 1000 °C were relatively very low. However, the diffraction peaks of the samples became sharper and sharper as the sintering temperature increased. According to Scherrer's formula $D = K\lambda/B\cos\theta$, the average grain sizes of LMO700, LMO800, LMO900, and LMO1000 were calculated to be 23 nm, 26 nm, 29 nm, and 30 nm, respectively. The above results indicate that, with the increase of the sintering temperature, the crystallization drive of the $LaMnO_{3+\delta}$ samples increases, the grain sizes increase, the crystallinity improves, and the manganese crystalline form becomes more complete.

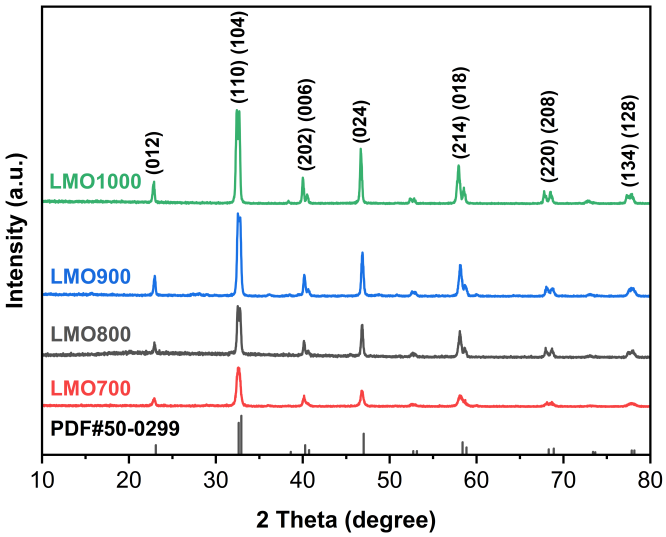

Figure 1. XRD patterns of $LaMnO_{3+\delta}$ samples prepared at different sintering temperatures

Figure 2 shows that the LMO700 was composed of particles with sizes of about 200 nm, which were stacked together, with irregular shapes, an uneven distribution, and obvious agglomeration among the particles, and the overall particles were in the form of polymers. As the sintering temperature increased, the particle size of LMO800 increased to about 300 nm, the edge of the particles became clearer; the particle size of LMO900 increased to about 500 nm with the bonding and agglomeration of the edge of particles, and the grains grew drastically. The growth trend of the particle size of the samples coincides with the change in the average grain size described in the previous XRD analysis. When the sintering temperature was increased to 1000 °C, the particle size in LMO1000 continued to increase, the agglomeration phenomenon became more serious, and the surface morphology changed from a loose granular polymer-like to a compact granular bonded-shaped mesh structure.

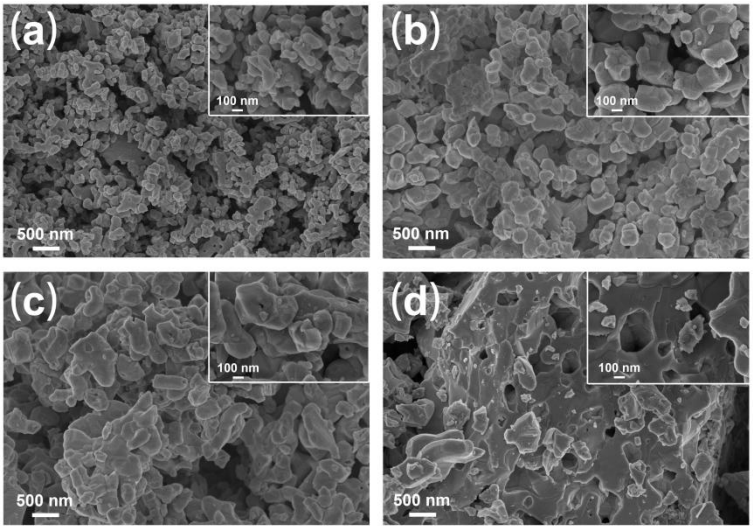

Figure 2. FESEM images of $LaMnO_{3+\delta}$ prepared at different sintering temperatures:(a) LMO700; (b) LMO800; (c) LMO900; (d) LMO1000

3.2. XPS analysis

Figure 3 (a–d) shows the XPS figures of the O 1s orbitals of $LaMnO_{3+\delta}$ after peak splitting fitting. It can be seen that the relative content of O_{ads} decreases with the increase of sintering temperature. The OER performance of electrocatalysts is weakened. In addition, the content of O_{ads} in transition metal oxides is linearly correlated with the concentration of oxygen vacancies, and the change of O_{ads} can be used to reflect the change of oxygen vacancy concentration in the lattice [4]. The higher content of O_{ads} means higher oxygen vacancies, which can promote the formation of electron-hole pairs and is conducive to the enhancement of the conductivity of the electrode. At this time, the lower the resistance of ions diffusing from the solution to the electrode surface, the stronger the charge transfer ability, and the better the OER performance [5,6].

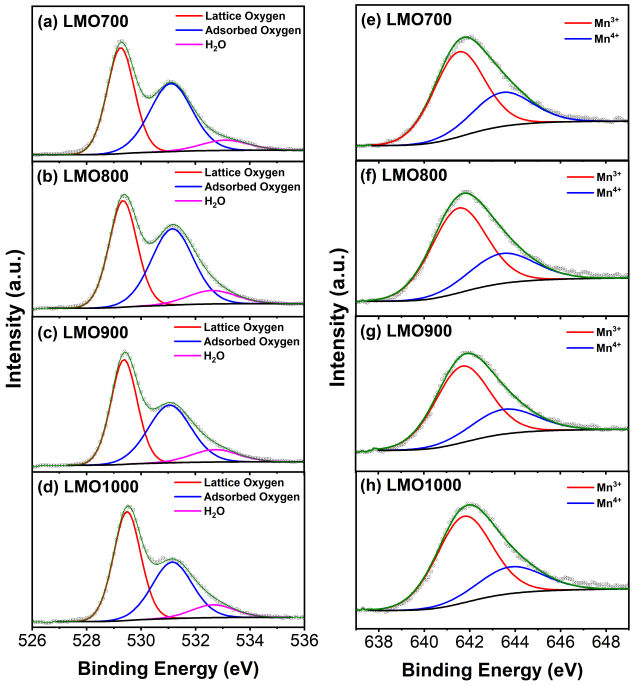

Figure 3. XPS patterns of $LaMnO_{3+\delta}$ prepared at different sintering temperatures: (a-d) O 1s; (e-h) Mn $2p_{3/2}$

Figure 3 (e-h) shows the XPS results of $LaMnO_{3+\delta}$ after peak splitting fitting to the Mn $2p_{3/2}$ orbitals. The Mn^{3+} /Mn^{4+} valence ratio increases from 2.15:1 to 2.75:1 with the increase of the sintering temperature. The increase in the content of Mn^{3+} will enhance the Mn^{3+}-O- Mn^{3+} super-exchange interaction and antiferromagnetism to some extent, which will then intensify the ferromagnetic/antiferromagnetic competition in the samples. In addition, according to the OER catalytic mechanism of Hardin [7], the oxidizability of Mn^{4+} is significantly higher than that of Mn^{3+}. When the LMO surface has a high content of Mn^{4+}, it will be favorable for the disproportionation reaction of HO^{2-} to produce oxygen during the reaction process, which will improve the OER performance of LMO. One can see that the LMO700 has the highest relative content of O_{ads} and Mn^{4+}, which endows it with good OER performance.

3.3. Magnetic studies

To investigate the influence of different sintering temperatures on the magnetic properties of $LaMnO_{3+\delta}$, we tested the M-T curves of LMO700 and LMO1000 under a magnetic field of 0.02 T (10-400 K) in ZFC and FC modes using VSM equipment, and the results are shown in **Figure 4**. The magnetization intensity of the two samples increased rapidly with the decrease of temperature below the Curie temperature of T_C, showing an obvious paramagnetic-ferromagnetic transition, which confirms that both samples demonstrate ferromagnetism. The values of T_C for LMO700 and LMO1000 were 173 K and 227 K, respectively, which imply that LMO1000 and LMO700 both had a relatively strong ferromagnetism. The T_C values of LMO700 and LMO1000 were 173 K and 227 K, respectively, implying that LMO1000 had a relatively strong ferromagnetic double exchange. The ferromagnetism of the LMO system is mainly attributed to the double exchange of Mn^{3+}-O-Mn^{4+}, and it is highly correlated with the Mn^{3+}/Mn^{4+} valence ratio. When the Mn^{3+} /Mn^{4+} valence ratio is close to 2:1, the ferromagnetic interaction in LMO is the strongest [8]. From the previous XPS analysis, when the sintering temperature is 700 ℃, the Mn^{3+}/Mn^{4+} valence ratio in LMO700 is 2.15:1 (the closest to 2:1) and should have the strongest ferromagnetic interactions theoretically. However, the M-T curve shows that the LMO1000 sample with a Mn^{3+} /Mn^{4+} valence ratio of 2.75:1 exhibits stronger ferromagnetism. When the oxygen vacancies in the system increase, it causes inhomogeneity of oxygen in the LMO lattice, which in turn disrupts this exchange mechanism and leads to higher spin disorder, weakening the ferromagnetism of the LMO [1].

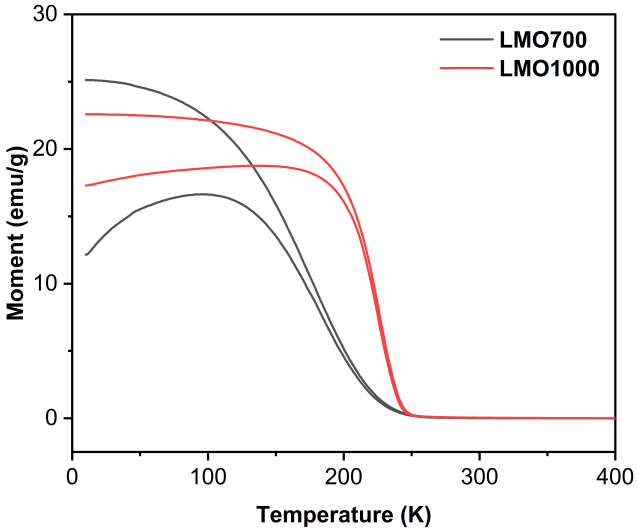

Figure 4. M-T curves of LMO700 and LMO1000

3.4. OER study

To investigate the effect of different sintering temperatures on the OER properties of $LaMnO_{3+\delta}$, we conduct LSV tests, and the results are shown in **Figure 5**. From **Figure 5(a)**, it can be seen that LMO700, LMO800, and LMO900 had similar onset potentials, whereas the onset potential of LMO1000 was quite different. For comparison, the current density values of $LaMnO_{3+\delta}$ samples at 1.7 V vs RHE were selected in this section to evaluate their electrocatalytic performance. As shown in **Figure 5(b)**, the current density of $LaMnO_{3+\delta}$ at 1.7 V vs RHE decreased gradually with the increase of sintering temperature, from 0.62 for LMO700 to 0.1 $mA \cdot cm^{-2}$, respectively.

Fig. 5(c) shows the Tafel plot obtained from LSV curve fitting, whose slope represents the magnitude of the charge transfer rate of the electrocatalyst. From Fig. 5(d), the LMO700 possesses the lowest Tafel slope of 366 $mV \cdot dec^{-1}$, which is much lower than that of 391 $mV \cdot dec^{-1}$ for LMO800, 410 $mV \cdot dec^{-1}$ for LMO900 and 466 $mV \cdot dec^{-1}$ for LMO1000, which implies that LMO700 has the highest charge transfer rate and relatively good OER reaction kinetics. As shown in Fig.2, the dense surface mesh structure and severe agglomeration of the particles of the LMO1000, and the relatively low surface O_{ads} and Mn^{4+} contents will conjointly reduce the surface-active sites of the catalysts, which in turn deteriorate the OER performance.

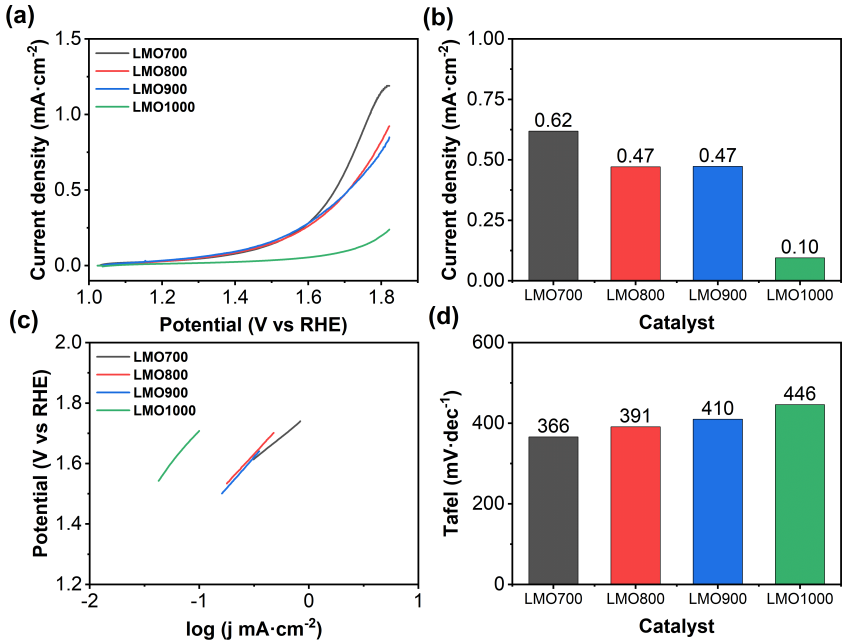

Figure 5. OER performance of $LaMnO_{3+\delta}$ prepared at different sintering temperatures: (a) LSV curve, (b) current density at 1.7 V *vs* RHE, (c) Tafel slope; (d) Tafel slope

The Cyclic voltammetry was used to calculate the capacitance of the bilayer to estimate the electrochemical active area (ECSA) of the catalyst. The voltage-current density plots as shown in Fig. 6(a-d) were obtained by performing CV tests on the catalysts with different scanning speeds, and then their fitting calculations resulted in the scanning speed-current density plots as shown in Fig. 6(e) (with a slope of $2C_{dl}$). From **Figure 6(f)**, it can be seen that the C_{dl} values of LMO700, LMO800, and LMO900 were not much different from each other, and they are all around 0.4 $mF \cdot cm^{-2}$. However, the C_{dl} value of LMO1000 is reduced to 0.12 $mF \cdot cm^{-2}$, indicating that its ESCA was drastically reduced with fewer active sites, which in turn is unfavorable for the OER-catalyzed reaction.

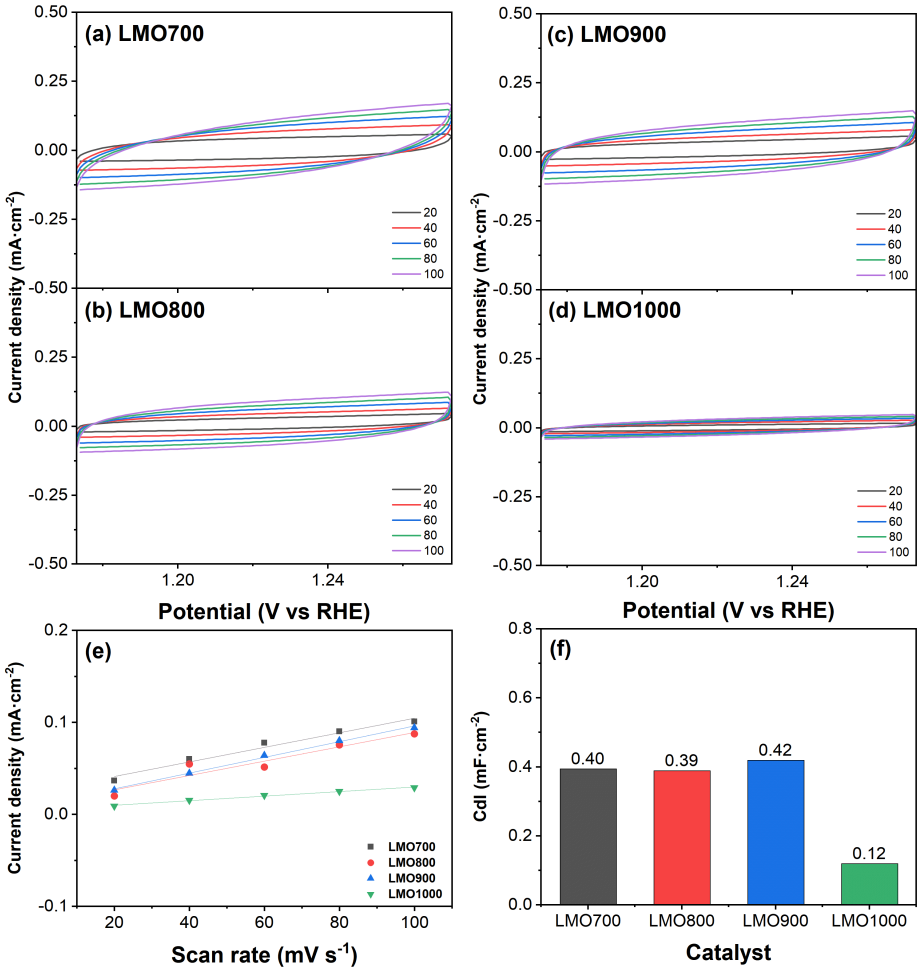

Figure 6. (a-d) Voltage-current density plots of $LaMnO_{3+\delta}$ prepared at different sintering temperatures at different sweep speeds; (e) corresponding sweep speed-current density plots; (f) the corresponding C_{dl}

4. Conclusion

The LMOs sintered in the air atmosphere were all tripartite ABO_3-type structures. With the increase of sintering temperature, the particle size of LMOs increased, and the content of O_{ads}, oxygen vacancies, and Mn^{4+} decreased, leading to the weakening of OER properties. The high concentration of oxygen vacancies in LMO700 disrupts the Mn^{3+}-O-Mn^{4+} double exchange interaction and intensifies the ferromagnetic/ antiferromagnetic competition. The macroscopic magnetism of LMO1000, T_C, T_{irr}, and T_f were higher than those of LMO700, which shows stronger ferromagnetism.

Funding

Open Foundation of Hubei Key Laboratory of Industrial Fume and Dust Pollution Control (Grants No.: HBIK2022-12) and Hubei Natural Science Foundation (Grant number: 2022CFC012).

Disclosure statement

The authors declare no conflict of interest.

References

[1] Kumari S, Mottaghi N, Huang C-Y, et al., 2020, Effects of Oxygen Modification on the Structural and Magnetic Properties of Highly Epitaxial $La_{0.7}Sr_{0.3}MnO_3$ (LSMO) Thin Films. Scientific Reports, 10(1): 1–11.

[2] Shen ZC, Qu M, Shi J, et al., 2022, Correlating the Electronic Structure of Perovskite $La_{1-x}Sr_xCoO_3$ with Activity for the Oxygen Evolution Reaction: The Critical Role of Co 3d Hole State. Journal of Energy Chemistry, 65: 637–645.

[3] Lu Z, Liu J, Feng J, et al., 2020, Synthesis of Single-Crystal $La_{0.67}Sr_{0.33}MnO_3$ Freestanding Films with Different Crystal-Orientation. APL Materials, 8(5): 051105.

[4] Yin YM, Xiong MW, Yang NT, et al., 2011, Investigation on Thermal, Electrical, and Electrochemical Properties of Scandium-Doped $Pr_{0.6}Sr_{0.4}(Co_{0.2}Fe_{0.8})_{(1-x)}Sc_xO_{3-\delta}$ as Cathode for IT-SOFC. International Journal of Hydrogen Energy, 36(6): 3989–3996.

[5] Mefford JT, Rong X, Abakumov AM, et al., 2016, Water Electrolysis on $La_{1-x}Sr_xCoO_{3-\delta}$ Perovskite Electrocatalysts. Nature Communications, 7: 11053.

[6] Ji Q, Bi L, Zhang J, et al., 2020, The Role of Oxygen Vacancies of ABO_3 Perovskite Oxides in the Oxygen Reduction Reaction. Energy & Environmental Science, 13(5): 1408–1428.

[7] Hardin WG, Mefford JT, Slanac DA, et al., 2014, Tuning the Electrocatalytic Activity of Perovskites Through Active Site Variation and Support Interactions. Chemistry of Materials, 26(11): 3368–3376.

[8] Camacho MCR, Valdés CFS, Curiel M, et al., 2020, Superparamagnetic State in $La_{0.7}Sr_{0.3}MnO_3$ Thin Films Obtained by rf-Sputtering. Scientific Reports, 10(1): 2568.